

EFFECT OF COMBINED TREATMENT METHODS ON THE CRYSTALLINITY AND SURFACE MORPHOLOGY OF KENAF BAST FIBERS

HARINI SOSIATI* and HARSOJO**

**Nanomaterials Research Group, Integrated Research and Testing Laboratory (LPPT), Gadjah Mada University, Yogyakarta 55281, Indonesia*

***Department of Physics, Faculty of Mathematics and Natural Sciences, Gadjah Mada University, Yogyakarta 55281, Indonesia*

Received February 24, 2013

Kenaf bast fibers were treated by combined methods with steam (steam-chemical-ultrasonic treatment) and without it (chemical-ultrasonic treatment). The crystallinity and morphological properties of these treated fibers were compared with the untreated ones. X-ray diffraction (XRD) and Fourier transform infrared (FTIR) spectroscopy were employed to appraise crystallinity. Morphological features were examined by scanning (SEM) and transmission (TEM) electron microscopies. The fibers treated with steam had a higher degree of crystallinity than those without steam treatments and the untreated fibers. However, steam pre-treatment tended to reduce the fiber surface roughness. The fibers treated without steam showed surprising morphology, which is characterized by the formation of nanofibers on the surface of microfibrils. Such morphology should enhance surface roughness and improve the performance of the corresponding composite.

Keywords: kenaf bast, steam pre-treatment, crystallinity, morphology

INTRODUCTION

Natural fiber reinforced polymer composite is a rapidly-growing functional material because of its low cost and weight, biodegradability and environmental friendliness. A single natural fiber consists of a bundle of cellulose microfibrils embedded in a soft matrix of mainly lignin and hemicelluloses; a low volume fraction of pectin serves to hold the microfibrils. The volume fraction of cellulose contained in the fiber, however, varies with the type of natural fiber.^{1,2}

Kenaf bast fiber is derived from a natural plant. In the last decade, much research interest has been focused on this fiber due to its potential in various applications. One potential application for the bast fiber is for reinforcing polymer composites used in interior automotive components,³⁻⁵ due to its superior flexural strength combined with its excellent tensile strength. It has been also used for membrane in filtration systems, owing to its ability to absorb nitrogen, phosphorus and heavy metals

contained in the soil and water,^{6,7} and also for absorbing carbon dioxide.⁸

Before fabricating the composite, it is quite necessary to treat the fiber to increase such properties as crystallinity and surface morphology. The treatment of the fiber basically removes the main non-cellulosic components, i.e. lignin, hemicelluloses and pectin, thereby isolating the cellulose. To achieve this end, various methods have been used to treat natural fibers. These include single, *viz.* acid hydrolysis,⁹ alkaline hydrolysis,¹⁰ mercerization,^{11,12} enzymatic treatment,¹³ and combination methods, *viz.* biotreatment-high shear refining-cryo-crushing,¹⁴ pulping-bleaching-acetylation-mechanical refining,¹⁵ pulping-bleaching-milling-cryocrushing-high pressure homogenizing,¹⁶ high pressure steam explosion technique (steam pre-treatment)-scouring-bleaching.¹⁷

A method that uses steam pre-treatment appears to be simple and effective. Research into the effect of the steam explosion technique on the properties of the fibers is not a new phenomenon. Vignon and coworkers¹⁸ showed that high pressure steam explosion is an effective method to degrade the pectin contained in the fiber and improve the mechanical properties of the fiber-reinforced polypropylene (PP) composite. This technique also enhances the crystallinity of the fiber.^{17,19} Immersing fibers in dilute alkaline solution prior steaming for 180 s at 220-500 °C resulted in complete solubilization of the non-cellulosic components. Thus, pure cellulose can be effectively isolated using high pressure steam explosion method. In addition, a mild steam treatment has been shown to increase the degree of crystallinity and improve the mechanical properties of the fibers to a greater extent than alkali treatment.²⁰ Recently, using bamboo fiber, Nguyen *et al.*²¹ compared steam explosion with the alkali method. While the former is more costly and required greater energy consumption, it carries no environmental effect; their experiment obtained no significant difference in the volume fraction of isolated cellulose or in the mechanical properties.

In this paper, we illustrate a simple method that employs a low pressure steam pre-treatment without the explosion technique, combined with chemical (scouring-bleaching) and ultrasonic treatments of kenaf bast fiber; this is compared with the same method but without steam pre-treatment. To date, steam pre-treatment has been considered to be important based on basic science and its application in polymer composite technology. Combination methods can be used to verify and understand their effect on the surface morphology of fibrillated cellulose and the degree of crystallinity, information which is lacking for kenaf bast fiber.

EXPERIMENTAL

Materials

The material used in this work was Indonesian cultivated kenaf variety KR-11, obtained from local Research Institution in Malang, East Java. Fibers of approximately 3-4 cm in length and 100 µm average diameter were selected from the middle part of the fiber, due to the higher tensile strength in the middle compared to the periphery. Before treatments, the fibers were dried in an oven at 70 °C for 30 minutes. This created an initial state designated as "raw-kenaf".

Treatment of kenaf fibers

Raw-kenaf fibers were treated by two combined methods, (1) without steam pre-treatment, i.e. chemical (scouring-bleaching)-ultrasonic treatment, and (2) with steam pre-treatment, i.e. steam-chemical (scouring-bleaching)-ultrasonic treatment.

Low pressure steam without explosion

Steam pre-treatment was conducted with a pressure cooker at 1.8 Bar (~117 °C) for 10, 20, 30, 60 and 90 minutes. The residence time in steam was measured after reaching the pressure of 1.8 Bar.

Scouring-bleaching

Scouring was done by soaking raw-kenaf fibers in 10 g/L NaOH and then heating at ~100 °C for 1 h with periodic stirring. Two g/L Teepol was added as surfactant in both scouring and bleaching solutions to reduce the surface tension of the fiber. The fiber:solution ratio was 1:250. The scoured fibers were washed in running distilled water and neutralized with 10 g/L acetic acid (CH₃COOH), then finally flushed with distilled water.

To remove the residual non-cellulosic components, the fibers were then bleached in a mixture of either 5 or 10 g/L NaOH and 20 or 100 ml/L H₂O₂ (Table 1) plus 2 g/L Teepol at ~100 °C for 1 h with periodic stirring. The bleached fibers were washed in running distilled water and then dried in an oven at 50 °C for 30 minutes. H₂O₂ has high oxidizing properties, which is good for bleaching. The volume ratio of H₂O₂ and NaOH used in bleaching was varied (Table 1).

Ultrasonic treatment (UT)

The bleached fibers were immersed in ethanol and treated in an ultrasonic cleaner (Power Sonic, LUC-405, Industrial BLT type) for various durations (see Table 1) operating at about 50 °C, 220 VAC and 50/60 Hz. During the treatment, the fibers were filtered and re-immersed in fresh ethanol before the next ultrasonic treatment. This step was repeated in each treatment for 1 h. This was done for two purposes, firstly to free the fibers from residual H₂O₂ and secondly to reduce the fiber size or to increase fibrillation.

Scanning and transmission electron microscopies (SEM and TEM)

The surface morphology and size of raw-kenaf and the treated fibers with steam and without it were characterized by scanning electron microscopy (SEM, INSPEX S50-FEI) with a W-filament operating at 15 kV and a working distance of 12 mm. Prior to SEM observation, the fiber specimens were surface coated with Au-Pd to increase the electrical conductivity of the specimens.

Table 1
Treatment conditions and analyses

Fiber specimen	Treatment				Analysis		
	Steam (1.8 Bar)	Scouring (~100 °C, 1 h)	Bleaching (~100 °C, 1 h)	Ultrasonic treatment (UT)	XRD	FTIR	SEM/TEM
Raw-kenaf	X	X	X	X	O	O	SEM
S10	X	O	X	X	O	X	SEM
S10-B52	X	10 g/L NaOH	5 g/L NaOH+ 20 ml/L H ₂ O ₂	X	O	X	SEM
S10-B101	X	10 g/L NaOH	10 g/L NaOH+ 100 ml/L H ₂ O ₂	1 h, 6 h, 28 h	O	O	SEM
S10-B102	X	10 g/L NaOH	10 g/L NaOH+ 20 ml/L H ₂ O ₂	X	O	X	SEM
ST10-SB101	10 min	same as above	10 g/L NaOH+ 100 ml/L H ₂ O ₂	1 h, 28 h	O	O	SEM
ST10-SB101	20 min	same as above	same as above	1 h	O	O	SEM
ST30-SB101	30 min	same as above	same as above	1 h	O	O	SEM
ST60-SB101	60 min	same as above	same as above	1, 4 h	O	X	SEM
ST90-SB101	90 min	same as above	same as above	1 h, 9 h	O	O	TEM

O: treatment or analysis was done, X: treatment or analysis was not done

In addition, the morphology of fiber treated with long steam pre-treatment for 90 minutes (specimen ST90-SB101-UT9, Table 1) was characterized with a TEM (JEM-1400) operating at 120 kV. The TEM specimen was prepared by placing a drop of ethanol containing the treated fibers that had been homogeneously dispersed on a carbon-coated grid.

X-ray diffraction (XRD)

The crystallinity of raw-kenaf and the treated fibers with steam and without it was semi-quantitatively analyzed from their XRD patterns (XRD, X'Pert Pro, PAN Analytical) under the following conditions. The specimens were irradiated with CuK α operating at 40 kV and 30 mA. XRD patterns were obtained at 2 theta from 10 to 50° at a counting rate of 0.05 %/s. The crystallinity index (*CI*) or degree of crystallinity of cellulose was determined empirically as follows.^{22,23}

$$CI = (I_{\max} - I_{\min})/I_{\max} \quad (1)$$

where I_{\max} is the height of the peak at 2θ between 22-24°, which represents both crystalline and amorphous cellulose; and I_{\min} is the height of the minimum at $2\theta = 19^\circ$, which represents the amorphous cellulose.

Fourier transform infrared spectroscopy

Fourier transform infrared (FTIR, Shimadzu) spectroscopy was performed to characterize the chemical functional groups in raw-kenaf and the treated fibers with steam and without it and to confirm the XRD results. Prior to the analysis, the fibers were shortened to about 100 μm . Approximately 1 mg fiber specimen was mixed with 200-300 mg KBr. The mixed powder was then pressed to form a translucent pellet through which the beam of the spectrometer could pass, and

subsequently analyzed in the transmittance mode within the range of 4000-500 cm^{-1} .

RESULTS AND DISCUSSION

Surface morphology

The cellulose microfibrils of the raw-kenaf fiber (Fig. 1 a) were bound in a bundle as a single fiber of approximately 100 μm average diameter (Fig. 1 a, insert A). The fiber was completely covered with a non-cellulosic membrane, which was wavy in shape because of the irregular arrangement of the microfibrils (Fig. 1 b).

An alkali solution is commonly used to break up the membrane. However, cellulose is resistant to strong alkali and oxidizing agents, whereas hemicelluloses are soluble in alkali and lignin in hot alkali.²⁴ After scouring with 10 g/L NaOH, the non-cellulosic components had been partly removed to clearly reveal the morphology of the microfibrils, including partial separation (Fig. 2). Residual non-cellulosic components on the surface of microfibrils are indicated by arrows (Fig. 2).

After scouring of fiber specimens S10-B52, S10-B101 and S10-B102 (Table 1), bleaching with one each different volume ratio of H₂O₂:NaOH resulted in different surface morphologies (Figs. 3 a, b and c, respectively). Residual non-cellulosic components were observed in all specimens. The average diameters of the fibers were relatively similar between treatments in the range of 10-20 μm . Pore-like surface damage on the fibers was apparent in S10-B52 (see arrows, Fig. 3 a), but not

in the other specimens. Upon close observation of the surface of the fibers, surface roughness of S10-B102 appeared to be the lowest, but fibrillation was higher than that of S10-B52 and S10-B101. These differences in morphology are probably related to the volume ratio of H₂O₂:NaOH used for bleaching: i.e. ~ (8:1) for S10-B52, ~ (21:1) for S10-B101 and ~ (4:1) for S10-B102. Referring to the high surface roughness, the volume ratio of ~ (21:1) used on fiber specimen S10-B101 is currently considered to be the preferred treatment, with steam and without it.

The ultrasonic treatment (UT) was used to remove the remaining bleaching solution, and to improve the fibrillation. Prolonging the duration of

this treatment on fiber specimen S10-B101 from 1 h to 6 h changed the surface morphology (Fig. 4). Fibrillation was expressed in the form of interesting microstructural evolution, which resulted in fiber diameter at micro- and nanoscales. Nanofibers formed on the surface of the microfibers, but the distribution across the entire area of fiber specimen was inhomogeneous. Microfiber of ~5 μm size had decomposed to nanofiber ≥100 nm. Good fibrillation had occurred, suggesting relative freedom from hemicelluloses and lignin. This observed morphology could be expected to increase surface roughness of the fiber and improve the properties of the corresponding composite.²⁵

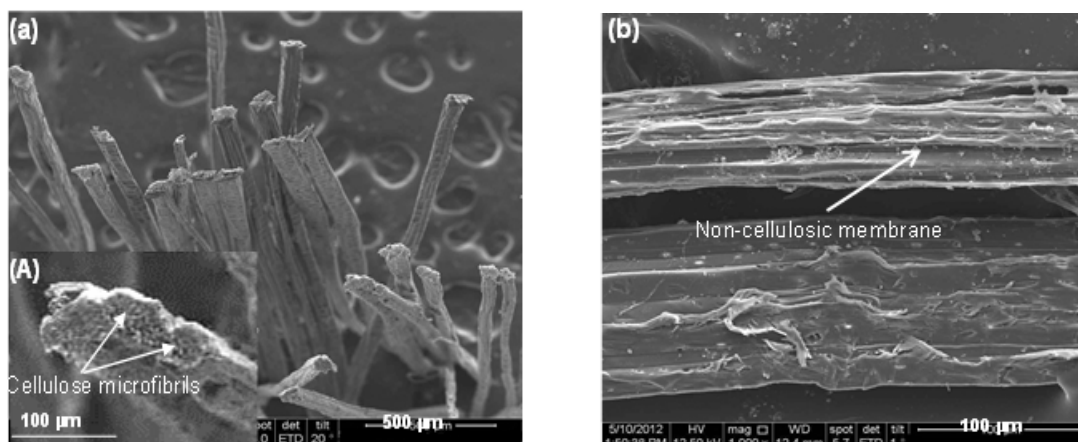


Figure 1: SEM micrographs of raw-kenaf observed cross-sectionally (a) and longitudinally (b). Insert (A) indicates a magnified image of a cross-section of fibers containing cellulose microfibrils

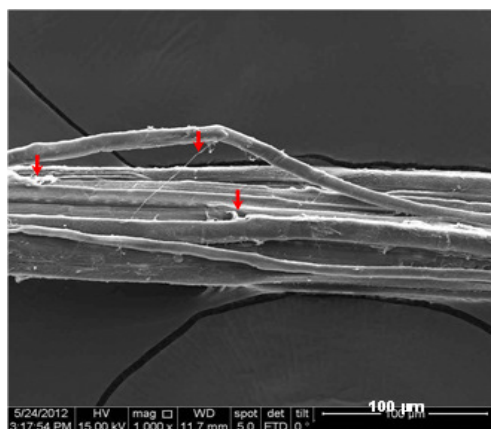


Figure 2: SEM micrograph of fiber specimen S10 (see Table 1) scoured with 10 g/L NaOH. The arrows point to non-cellulosic components on the surface of microfibrils

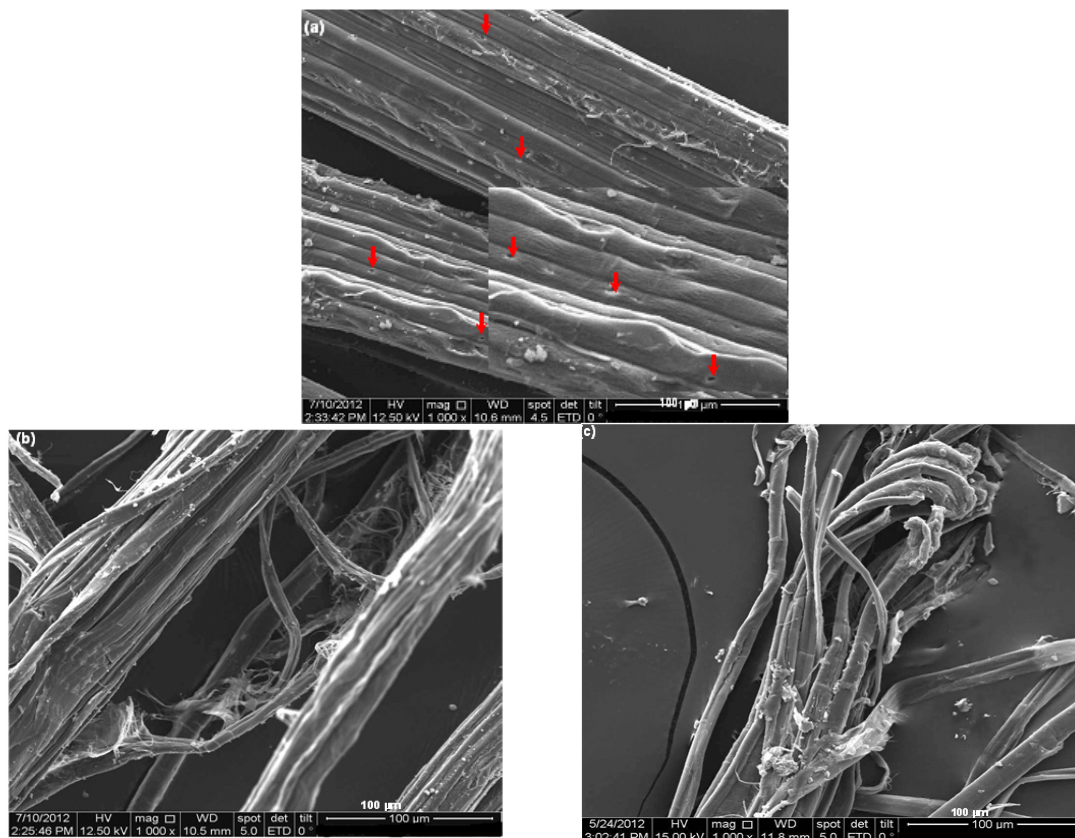


Figure 3: SEM micrograph of fiber specimens (a) S10-B52, (b) S10-B101 and (c) S10-B102 showing different surface morphologies due to different volume ratio of NaOH:H₂O₂ (see Table 1)

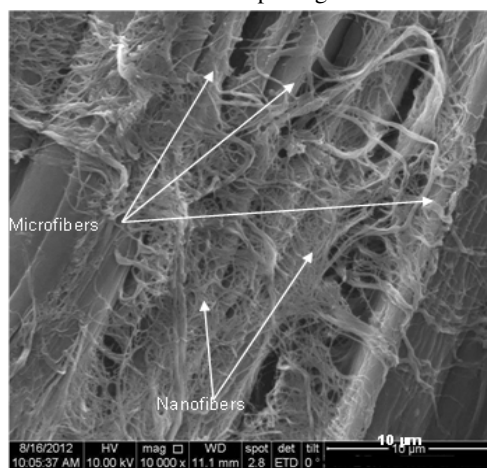


Figure 4: SEM micrograph of fiber specimen S10-B101-UT6

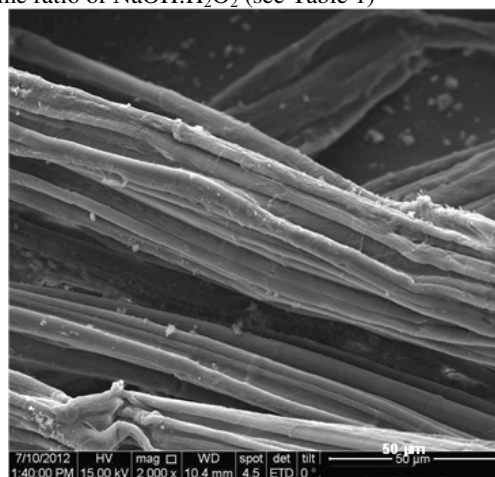


Figure 5: SEM micrograph of fiber specimen ST10-SB101

Steam pre-treatment for 10, 20 and 30 min on fiber specimen S10-B101, followed by UT for 1 hour was designated as fiber specimens ST10-SB101-UT1, ST20-SB101-UT1 and ST30-SB101-UT1 (Table 1). The UT treatment

resulted in higher fibrillation with individual fibers of about 8 µm in size, as represented in Fig. 5. The micrograph also shows that steam pre-treatment encouraged the cleavage of the non-cellulosic components, but retained the crystallinity of the

microfibrils. Increasing the duration of steam pre-treatment for 20 and 30 minutes had no effect on surface morphology properties.

Steaming for 60 min and UT for 4 h also resulted in micro- and nanoscale fibers (Fig. 6; fiber specimen ST60-SB101-UT(4), see Table 1). Fibrillation was observed, but the morphology of the fiber surface was dissimilar to that of specimen S10-B101-UT(6), as part of the fiber had completely fibrillated to nanofibers (Fig. 6). Steaming for 60 min possibly accelerated the fibrillation. Increasing steam residence time to 90 min and UT to 9 hours after bleaching (see fiber specimen ST90-SB101-UT9 in Table 1) made the fibers more brittle and easier to separate from each other. Visual observation indicated that as residence time in steam lengthens, the brittleness of fibers will tend to become higher and fiber length shorter. A TEM image of ST90-SB101-UT9 revealed that fiber diameter varied from <100 nm to >100 nm with uniform distribution (Fig. 7).

Crystallinity

XRD patterns of raw-kenaf and treated fibers with steam and without it were examined after scouring (S10), after scouring-bleaching (S10-B101), after steam-scouring (ST10-S10) and after steam-scouring-bleaching (ST10-SB101) (Fig. 8) and for steam treated fibers, after different

steam residence times (Fig. 9); peak positions and degree of crystallinity (see Equation 1) are summarized in Table 2. To accurately identify the peak positions, Gaussian peak software Origin 8 was used.

The position of peak 1 on all specimens is relatively similar, whereas that of peak 2 measured as maximum intensity, for treated fiber with steam and without it, tends to gradually shift to higher 2 theta, which is close exactly to the position of maximum intensity (I_{002} lattice reflection) of native cellulose at 2 theta 22.841°, compared to raw-kenaf. This is consistent with the gradual increase of their crystallinity degree, suggesting that a part of the non-cellulosic components was slightly removed due to scouring with alkali solution and scouring-bleaching with NaOH and H₂O₂. Fiber specimens treated with steam (ST10-SB101, ST20-SB101, ST30-SB101, ST60-SB101 and ST90-SB101) show similar XRD patterns and the position of peak 2 at 2 theta 22.55°. The slightly higher degree of crystallinity of treated fiber with steam and without it, summarized in Table 2, than that of raw-kenaf is possibly due to the low concentration of NaOH used for chemical treatment. However, the surface morphology of the treated fibers with steam and without it showed a clear difference, compared with that of raw-kenaf, as described in the previous section.

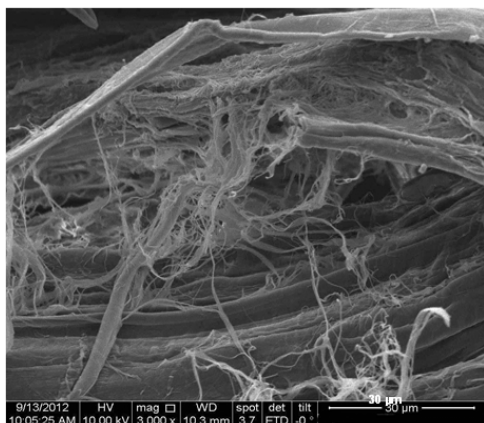


Figure 6: SEM micrograph of fiber specimen ST60-SB101-UT4

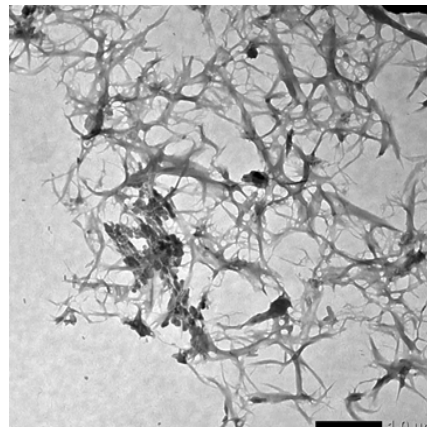


Figure 7: TEM micrograph of fiber specimen ST90-SB101-UT9

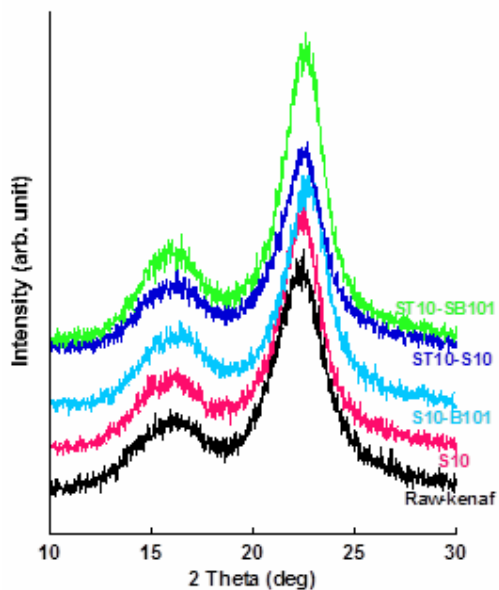


Figure 8: XRD patterns of raw-kenaf and treated fiber with steam and without it

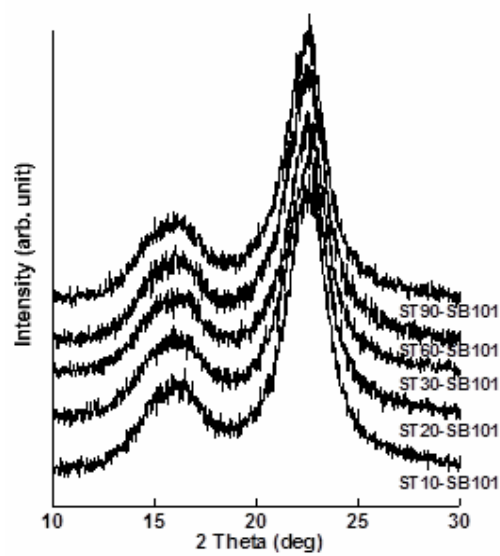


Figure 9: XRD patterns of treated fiber with steam for various durations

Table 2
Peak position and crystallinity degree of raw-kenaf and treated fibers

Sample	Position at 2 theta (degree)		Crystallinity degree (%)
	Peak 1	Peak 2	
Raw-kenaf	16.16	22.33	81.193
S10	16.16	22.44	83.101
S10-B101	16.16	22.77	84.124
ST10-S10	16.16	22.55	85.844
ST10-SB101	16.16	22.55	89.049
ST20-SB101	16.16	22.55	85.401
ST30-SB101	16.16	22.55	88.372
ST60-SB101	16.16	22.55	85.872
ST90-SB101	16.16	22.55	87.153

The degree of crystallinity of raw-kenaf was relatively high. The KR 11-based kenaf bast was from a superior variety and harvested about 120 days after planting. The chemical composition of kenaf is a function of the growing season; cellulose content increases with age.²⁶ The high degree of crystallinity found in this experiment is comparable with that obtained from kenaf varieties viz KR-11 (81.19), C-108 (78.91), Tinung-1 (73.94%), Everglade 45-49 (78.32), and Everglade 41 (80.43%), all of almost similar age.²⁶ All these varieties appear to contain a relatively low level of non-cellulosic components. Thereby, in this

experiment a high concentration of NaOH is not required to treat the fibers.

In addition, FTIR spectroscopy was used to characterize the chemical compounds in the fiber specimens as the absorbance spectra attributed to cellulose as crystalline phase, hemicelluloses and lignin as amorphous phases, the main components contained in the fiber specimens (Tables 3 and 4). The peaks related to cellulose, hemicelluloses and lignin are summarized globally in Table 3 and in detail in Table 4.

Figure 10 displays FTIR spectra obtained from raw-kenaf, the treated fiber without steam (S10-B101-UT1) and with steam (ST10-SB101).

The absorption peaks at 1740, 1627 and 1242 cm^{-1} , which indicate lignin and hemicelluloses^{10,16,17,33,34} were absent in the treated fiber specimens; however an absorption peak at 1327 cm^{-1} ,

corresponding to lignin, remained present in these fibers. Thus most of the hemicelluloses were removed by the applied treatments, but some lignin remained.

Table 3
Infrared band assignments for cellulose, hemicelluloses and lignin

Wavenumber (cm^{-1})	Assignment
3600-3100	Stretching of OH-groups on cellulose molecules ^{15,27}
2990-2850	C-H stretching vibration ²⁸
1750-1700, 1513	C=O stretching of carbonyl related to hemicelluloses and lignin ^{10,17}
1646-1632	Absorbed water ^{28,29}
1600-1500	Aromatic skeletal vibration corresponded to the presence of pure hemicellulose and lignin ¹⁰
1434-1421	A symmetric CH_2 bending vibration attributed to crystalline cellulose ^{27,28,30}
1239	C-O stretching of the aryl group in lignin ³¹
1431, 1372, 1319, 1165, 1059 and 896	Typical of pure cellulose ^{17,32}

Table 4
Identification of peaks^{33,34}

Wavenumber (cm^{-1})	Substances
<u>Clear peaks:</u> 1643, 1427 and 899	Cellulose
<u>Small peaks or shoulders:</u> 1367, 1319, 1337, 1284, 1203, 1161, 1119, 1114 and 999	
<u>Clear peaks:</u> 1646, 1563, 1044 and 899	Hemicelluloses
<u>Small peaks or shoulders:</u> 1508, 1461, 1420, 1252, 1212, 1164 and 990	
<u>Clear peaks:</u> 1697, 1603, 1514 and 837	Lignin
<u>Small peaks or shoulders:</u> 1457, 1423, 1327, 1281 and 1034	

The degree of crystallinity increases with the level of isolation of cellulose. The IR crystallinity index of cellulose from natural fibers³⁰ can be estimated from the ratio of absorbance intensity at 1427 and 895 cm^{-1} , which are respectively assigned to CH_2 bending mode^{27,28,30} and deformation of anomeric CH;³⁵ i.e. (A_{1427}/A_{895}). This is used to confirm the XRD results. Accordingly, the IR crystallinity index of fiber specimens S10-B101-UT1 and ST10-SB101 is 2.66 and 1.16, respectively. This indicates that the crystallinity of the fiber specimen treated without steam was higher than that with steam, whereas the degree of crystallinity estimated by XRD indicated the opposite. This difference can be ascribed to the

1 h UT applied to specimen S10-B101 before FTIR analysis. Thus, UT after bleaching played a crucial role in improving the crystallinity of the cellulose fiber.

Changing the duration of UT from 1 h (S10-B101-UT1) to 6 h (S10-B101-UT6) resulted in very little difference in crystalline index, 2.66 and 2.69, respectively (Fig. 11). After UT of 28 h, however, the FTIR spectrum became quite different and the crystallinity index was 1.30. Shoulder peaks at 1026, 1157, 1342, 1628, 1759 cm^{-1} were also observed, and the peak related to cellulose at 1427 cm^{-1} was lower. Thus long UT may be associated with damage to the structure of cellulose microfibrils.

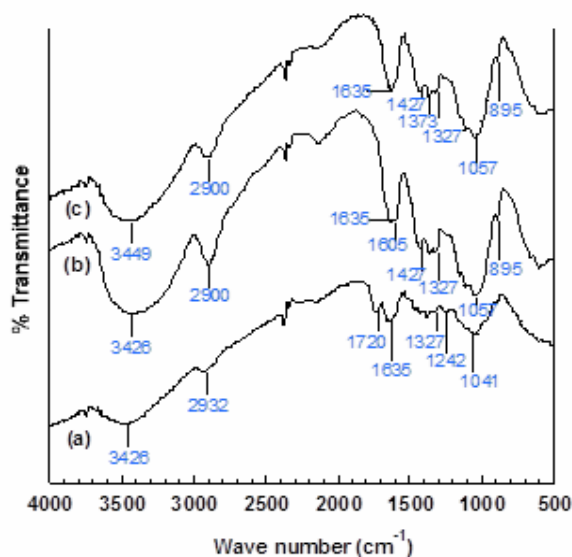


Figure 10: FTIR spectra of (a) raw-kenaf, (b) fiber specimen S10-B101-UT1 and (c) fiber specimen ST10-SB101

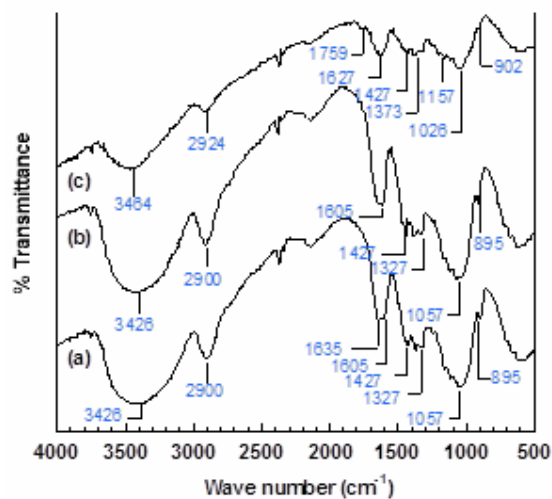


Figure 11: FTIR spectra of (a) fiber specimen S10-B101-UT1, (b) fiber specimen S10-B101-UT6 and (c) fiber specimen S10-B101-UT28

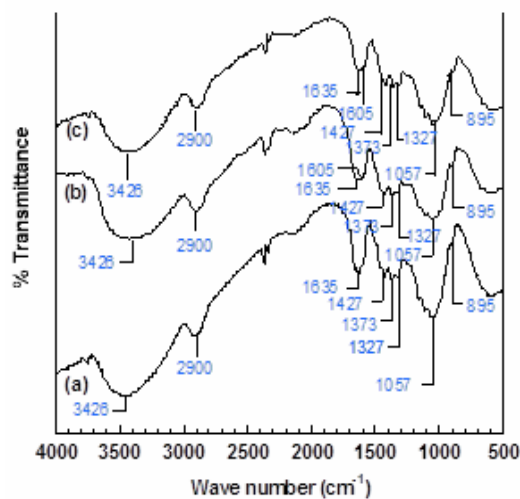


Figure 12: FTIR spectra of (a) fiber specimen ST10-SB101, (b) fiber specimen ST10-SB101-UT9 and (c) fiber specimen ST10-SB101-UT28

Long UT applied on fiber specimen ST10-SB101 (without UT), 9 h (ST10-SB101-UT9) and 28 h (ST10-SB101-UT28) (see Table 1) shows the FTIR spectra presented in Fig. 12. The crystallinity index of these fiber specimens increased from 1.16 (ST10-SB101) to 1.84 (ST10-SB101-UT9) and 2.87 (ST10-SB101-UT28). The crystallinity index 2.87 (ST10-SB101-UT28) was higher than that of

fiber specimens treated without steam, 2.66 (S10-B101-UT1), 2.69 (S10-B101-UT6) and 1.3 (S10-B101-UT28). Thus partial removal of the non-cellulosic components by steaming for 10 minutes before the chemical treatment followed by long UT is very effective in increasing crystallinity. Long UT without steam, however, provides no benefit. The functional reason for the difference in

crystallinity index between S10-B101-UT28 (1.3) and ST10-SB101-UT28 (2.87) remains unclear.

Relationship between surface morphology and the degree of crystallinity of cellulose microfibrils

Surface morphology and crystallinity of the cellulose fiber are two of some important factors that increase the performance of the corresponding composite. Fibers with a high degree of crystallinity may contain a high volume fraction of crystalline cellulose, but the fiber surface appeared to be relatively smooth with low surface roughness, e.g. fiber specimen ST10-SB101-UT1 (Fig. 5). A high content of cellulose indicates a high OH-group content, suggesting the fiber is more hydrophilic, a property that is incompatible with the hydrophobic nature of the matrix material used in the fabrication process of the fiber composite.

Fibers with a high degree of crystallinity lead to higher tensile strength of the fiber and thus to improved mechanical properties of the corresponding composite.^{16,20} High surface roughness of the fiber has also played a significant role in enhancing the bonding strength between fiber and matrix.^{36,37} Reducing fibers that combine a high degree of crystallinity with surface roughness is not simple, as they tend to be inversely related. Thereby, optimization of both properties is quite necessary.

In this study, we have produced fibers that have remarkable surface morphology, including nanoscaled fibers formed on the surface of microfibers, e.g. S10-B101-UT6 (Fig. 4). Such morphology is expected to increase surface roughness. The relatively high crystallinity index and surface roughness of S10-B101-UT6 would be expected to provide good performance of the corresponding composite.

CONCLUSION

The morphology and crystallinity of raw kenaf and treated fibers with steam and without it under low pressure were characterized by SEM, XRD and FTIR. Fibers treated by the combined steam-chemical-ultrasonic method resulted in a higher degree of crystallinity and better fibrillation than by chemical-ultrasonic only. Steaming on raw

fiber promoted cleavage of the non-cellulosic components and accelerated the removal of the non-cellulosic components and the fibrillation process. Steaming for >30 min provided no further enhancement of the degree of crystallinity. A high degree of crystallinity after steam pre-treatment reduced surface roughness.

Relatively high crystallinity and micro- and nanodiameter fibers produced without steam resulted in a morphology where nanodiameter fibers formed on the surface of microfibers. This property is expected to increase surface roughness and improve the performance of the corresponding composite.

ACKNOWLEDGEMENTS: The authors acknowledge the INCENTIVE PROGRAM OF CLUSTER RESEARCH, GadjahMada University for funding this project (LPPM UGM/3829/BID.III/2012). The authors also would like to thank the students Supatmi, Wijayanti Dwi Astuti, Ma'arif and Ar Rohim for help in fiber treatments.

REFERENCES

- 1 M. P. Westmann, L. S. Fifield, K. L. Simmons, S. G. Ladda and T. A. Kafentzis, "Natural Fiber Composites: A Review", March, 2010, available on http://www.pnl.gov/main/publications/external/technical_reports/PNNL-19220.pdf
- 2 G. Siqueria, J. Bras and A. Dufresne, *Polymer*, **2**, 728 (2010).
- 3 J. Holbery and D. Houston, *JOM*, **32(11)**, 80 (2006).
- 4 T. Nishimura, *Journal-Society of Automotive Engineers of Japan*, **60**, 100 (2006).
- 5 M. Zampaloni, F. Pourboghra, S. A. Yankovich, B. N. Rodgers, J. Moore *et al.*, *Composites Part A*, **38**, 1569 (2007).
- 6 K. Abe and Y. Ozaki, *Soil Sci. Plant Nutr.*, **44(4)**, 599 (1998).
- 7 C. L. Radiman, S. Widyaningsih and S. Sugesty, *J. Membrane Sci.*, **315**, 141 (2008).
- 8 S. Amaducci, M. T. Amaducci, M. Benati and G. Venturi, *Ind. Crop. Prod.*, **1(2-3)**, 179 (2000).
- 9 Q. Xiang, Y. Y. Lee, P. Q. Pettersson and R. W. Torquet, *Appl. Biochem. Biotechnol.*, **105-108**, 505 (2003).
- 10 J. I. Morán, V. A. Alvares, V. P. Cyras and A. Vasques, *Cellulose*, **15(1)**, 149 (2008).
- 11 E. Dinand, M. Vignon, H. Chanzy and L. Heux, *Cellulose*, **9**, 7 (2000).
- 12 K. C. C. Carvalho, D. R. Mulinari, H. C. Voorwald and M. O. H. Cioffi, *BioResources*, **5(2)**, 1143 (2010).

- ¹³ M. Herriksson, G. Herriksson, L. A. Berglarad and T. Lindstrom, *Eur. Polym. J.*, **43**(8), 3434 (2007).
- ¹⁴ S. Janardhnan and M. M. Sain, *BioResources*, **1**(2), 176 (2006).
- ¹⁵ M. Jonoobi, J. Harun, P. M. Tahir, L. K. Zaini, S. S. Azryet *et al.*, *BioResources*, **5**(4), 2556 (2010).
- ¹⁶ M. Jonoobi, J. Harun, A. Shakeri, M. Misra and K. Oksman, *BioResources*, **4**(2), 626 (2009).
- ¹⁷ M. M. Ibrahim, F. A. Agblevor and W. K. El-Zawawy, *BioResources*, **5**(1), 397 (2010).
- ¹⁸ M. R. Vignon, D. Dupeyre and C. Garcia-Jaldon, *Bioresource Technol.*, **58**(2), 203 (1996).
- ¹⁹ W. G. Glasser and R. S. Wright, *Biomass Bioenerg.*, **14**, 219 (1998).
- ²⁰ S. S. Munawar, K. Unemura, F. Tanaka and S. Kawai, *J. Wood Sci.*, **53**(6), 481 (2007).
- ²¹ T. P. Nguyen, T. Fuji, B. Chuong and K. Okubo, *J. Mater. Sci. Res.*, **1**(1), 144 (2012).
- ²² L. Segal, L. Creely, A. E. Martin and C. M. Conrad, *Text. Res. J.*, **29**, 786 (1959).
- ²³ S. Janardhan and M. Sain, *Bioresources*, **6**, 1242 (2011).
- ²⁴ Private discussions.
- ²⁵ T. Nishino, K. Hirao, M. Kotera, K. Nakamae and H. Inagaki, *Composites Sci. Technol.*, **63**, 1281 (2003).
- ²⁶ R. M. Rowell and H. P. Stout, "Jute and Kenaf: Handbook of Fiber Chemistry", 3rd ed., CRS Press, 2006, pp. 414-416, available on http://www.fpl.fs.fed.us/documnts/pdf2007/fpl_2007_rowell004.pdf
- ²⁷ D. Ciolacu, F. Ciolacu and V. I. Popa, *Cellulose Chem. Technol.*, **45**(1-2), 13 (2011).
- ²⁸ N. Nosbi, H. M. Akil, Z. A. M. Ishak and A. Abu Bakar, *BioResources*, **6**(2), 950 (2011).
- ²⁹ S. Kokot, A. T. Nguen, L. Rintoul, *Appl. Spectrosc.*, **51**, 387 (1997).
- ³⁰ Y. Kataoka and T. Kondo, *Macromolecules*, **31**, 760 (1998).
- ³¹ M. Troedec, D. Sedan, C. Peyratout, J. Bonnet, A. Smith *et al.*, *Compos. Part A-Appl. S.*, **39**(3), 514 (2008).
- ³² E. Dinand, M. Vignon, H. Chanzy and L. Heux, *Cellulose*, **9**, 7 (2002).
- ³³ P. K. Adapa, C. Karunakaran, L. G. Tabil and G. J. Schoenau, *The Canadian Society for Bioengineering: CSBE/SCGAB 2009 Annual Conference, Rodd's Brudenell River Resort, Prince Edward Island*, 12-15 July, 2009, pp. 1-21.
- ³⁴ P. K. Adapa, C. Karunakaran, L. G. Tabil and G. J. Schoenau, *Agric. Eng. Int.*, **9**, 1 (2009).
- ³⁵ J. Blackwell, P. D. Vasko and J. L. Koenig, *J. Appl. Phys.*, **41**, 4375 (1970).
- ³⁶ X. Li, L. G. Tabil, S. Panigrahi, *J. Polym. Environ.*, **15**, 25 (2007).
- ³⁷ N. Chawla, J. W. Holmess and J. F. Masisfield, *Mater. Charact.*, **35**, 199 (1995).